J|A|C|S
ARTICLES
Published on Web 08/31/2002

Colloidal Synthesis and Self-Assembly of $CoPt_3$ Nanocrystals

Elena V. Shevchenko, Dmitri V. Talapin, Andrey L. Rogach, Andreas Kornowski, Markus Haase, and Horst Weller*

Contribution from the Institute of Physical Chemistry, University of Hamburg, D-20146 Hamburg, Germany

Received February 19, 2002

Abstract: Reduction of platinum acetylacetonate and thermodecomposition of cobalt carbonyl in the presence of 1-adamantanecarboxylic acid were employed in different coordinating mixtures to produce monodisperse, highly crystalline $CoPt_3$ nanoparticles. The mean particle size can be varied from 1.5 to 7.2 nm by controlling the reaction conditions and the type of coordinating mixture. As-synthesized $CoPt_3$ particles represent single crystal domains and have chemically disordered face-centered cubic (fcc) structure. Nearly spherical $CoPt_3$ nanocrystals were found to assemble into two- (2D) and three-dimensional (3D) structures. An AB_5 type superlattice is observed by TEM after mixing two nanoparticle samples with different mean sizes. Slow precipitation led to the formation of facetted colloidal crystals with sizes up to 20 μm.

Introduction

Magnetic nanosized materials attract growing interest because of their potential in ultrahigh-density magnetic recording systems.[1] As in the nanometer size regime the magnetic properties become strongly dependent on the particle size,[2] synthetic methods yielding monodisperse magnetic nanocrystals of tunable size are extremely important. Several successful synthetic approaches for Fe,[3] Co,[4] FePt,[5] and $Fe_xCo_yPt_{100-x-y}$[6] nanocrystals were recently developed providing particles of controllable shapes and narrow size distributions. They are currently under investigation with the goal of understanding both the mechanism of formation of monodisperse nanocrystals and the influence of size and shape on their magnetic behavior. Recently, the preparation of polydisperse Co−Pt alloy nanoparticles of ∼2 nm from organometallic precursors in the presence of polymer was reported.[7] Because of strong perpendicular magnetic anisotropy of bulk Co−Pt alloys[8] and their high chemical stability,[9] these materials might be especially suitable for magnetooptical storage media.[10]

In this paper we report on the colloidal synthesis of monodisperse $CoPt_3$ nanocrystals of various distinct sizes. The key point of the synthesis is the use of a novel efficient stabilizer, 1-adamantanecarboxylic acid. Self-assembly of $CoPt_3$ nanocrystals into two-dimensional (2D) and three-dimensional (3D) superstructures as well as the preparation of colloidal crystals (∼10−20 μm in size) with the nanocrystals as building blocks is also reported.

Experimental Section

Chemicals. Toluene, methanol, *n*-hexane (all anhydrous, Aldrich), diphenyl ether (99%, Alfa Aesar), *n*-tetradecylphosphonic acid (*n*-TDPA, 98%, Alfa Aesar), 1,2-hexadecandiol (90%, Fluka), 1-adamantanecarboxylic acid (ACA, 99%, Fluka), 1,2-dichlorobenzene (99%, Acros Organics), cobalt carbonyl ($Co_2(CO)_8$, stabilized with 1−5% of hexane, Strem), and platinum(II)−acetylacetonate ($Pt(acac)_2$, 98%, Strem) were of the highest purity available and used as received. Hexadecylamine (HDA; Merck) was purified by a vacuum distillation.

Synthesis of $CoPt_3$ Nanocrystals. $CoPt_3$ nanocrystals were formed via a modified "polyol" process[5] in a high-boiling coordinating solvent. During particle formation, $Pt(acac)_2$ was reduced by a long-chain 1,2-diol and cobalt carbonyl was thermally decomposed. The synthesis was carried out using standard Schlenk line technique under dry argon.

Cobalt stock solution was freshly prepared before synthesis by dissolving 0.043 g of $Co_2(CO)_8$ in 0.4 mL of 1,2-dichlorobenzene at room temperature under airless conditions.

* Corresponding author. Fax: +49-40-428383452. E-mail: weller@chemie.uni-hamburg.de.

(1) (a) Zeper, W. B.; Greidaus, F. J. A. M.; Garcia, P. F.; Fincher C. R. *J. Appl. Phys.* **1989**, *65*, 4971. (b) Hashimoto, S.; Ochiai, Y.; Aso, K. J. *Appl. Phys.* **1990**, *67*, 2136. (c) Hashimoto, S.; Maesaka, A.; Fujimoto, K.; Bessho, K. *J. Magn. Magn. Mater*. **1993**, *121*, 471. (d) Black, C. T.; Murray, C. B.; Sandstrom, R. L.; Sun, S. *Science* **2000**, *290*, 1131.
(2) Leslie-Pelecky, D. L.; Rieke, R D. *Chem. Mater*. **1996**, *8*, 1770.
(3) Park, S.-J.; Kim, S.; Lee S.; Khim, Z.; Char, K.; Hyeon, T. *J. Am. Chem. Soc*. **2000**, *122*, 8581.
(4) (a) Dinega, D. P.; Bawendi, M. G. *Angew. Chem., Int. Ed. Engl*. **1999**, *38*, 1788. (b) Sun, S.; Murray, C. B. *J. Appl. Phys*. **1999**, *85*, 4325. (c) Puntes, V. F.; Krishan, K. M.; Alivisatos, A. P. *Appl. Phys. Lett.* **2001**, *78*, 2187. (d) Puntes, V. F.; Krishan, K. M.; Alivisatos, A. P. *Science* **2001**, *291*, 2115.
(5) Sun, S.; Murray, C. B.; Weller, D.; Folks, L.; Moser, A. *Science* **2000**, *287*, 1989.
(6) Chen, M.; Nikles D. E. *Nano Lett.*, in press.
(7) (a) Ould Ely, T.; Pan, C.; Amiens, C.; Chaudret, B.; Dassenoy, F.; Lecante, P.; Casanove, M.-J.; Mosset, A.; Respaund, M.; Broto, J.-M. *J. Phys. Chem. B* **2000**, *104*, 695. (b) Park, J. I.; Cheon, J. *J. Am. Chem. Soc*. **2001**, 123, 5743.
(8) Weller, D.; Brändle, H.; Chappert, C. *J. Magn. Magn. Mater*. **1993**, *121*, 461.
(9) Tyson, T. A.; Conradson, S. D.; Farrow, R. F. C.; Jones, B. A. *Phys. Rev. B* **1996**, *54*, R3702.
(10) (a) Grange, W.; Maret, M; Kappler, J.-P.; Vogel, J.; Fontaine, A.; Petroff, F.; Krill, G.; Rogalev, A.; Coulon, J.; Finazzi, M.; Brookes, N. *Phys. Rev. B* **1998**, *58*, 6298. (b) Weller, D.; Brändle, H.; Gorman, G.; Lin, C.-J.; Notarys, H. *Appl. Phys. Lett*. **1992**, *61*, 2726. (c) Lin, C.-J.; Gorman, G. L. *Appl. Phys. Lett*. **1992**, *61*, 1600. (d) Shapiro, A. L.; Rooney, P. W.; Tran, M. Q.; Hellman, F.; Ring, K. M.; Kavanagh, K. L.; Rellinghaus, B.; Weller, D. *Phys. Rev. B* **1999**, *60*, 12826. (e) Chang, G.; Lee, Y.; Rhee, J.; Lee, J.; Jeong, K.; Whang, C. *Phys. Rev. Lett*. **2001**, *87*, 067208−1.

10.1021/ja025976l CCC: $22.00

Table 1. Experimental Conditions Applied for Preparation of $CoPt_3$ Nanocrystals[a]

coordinating solvent mixtures	temp of injection, °C	temp of reacn, °C	time of reacn	comments
HDA diphenyl ether	100	268−290	1 min	spherical nanocrystals of ∼46 nm size, some amount of nanowires
			40 min	spherical nanocrystals of ∼46 nm size, some amount of nanowires
			3 h	almost only spherical nanocrystals of ∼46 nm
	170	230	40 min	spherical nanocrystals of 4.0 nm
		268		spherical nanocrystals of 4.0 nm
	220	230		spherical nanocrystals of 2.6 nm
TDPA diphenyl ether	100	255	40 min	spherical nanocrystals of ∼35 nm
	170	255		spherical nanocrystals of ∼3.6 nm
HDA, 1-hexadecanol	100	220	40 min	spherical nanocrystals of ∼1.52 nm
	170			

[a] ACA was used as stabilizer throuout.

In a typical synthesis, 0.033 g of $Pt(acac)_2$, 0.13 g of 1,2-hexadecandiol, and 0.084 g of 1-adamantanecarboxylic acid were dissolved in a mixture of coordinating solvents and heated to 65 °C in a three-neck flask until a clear solution was formed. Three types of coordinating mixtures were used: (i) diphenyl ether (2.0 mL) and HDA (4.0 g), (ii) diphenyl ether (6.0 mL) and TDPA (0.04 g), and (iii) HDA (0.04 g) and 1-hexadecanol (6.0 g). To produce $CoPt_3$ nanocrystals, the reaction mixture was heated either to 100 or to 170 °C and cobalt stock solution was injected into the flask under vigorous stirring. $CoPt_3$ nanocrystals of 2.6 nm diameter were prepared by injection of a mixture of cobalt stock solution, 1,2-hexadecandiol, and 1.5 mL of diphenyl ether into an HDA-diphenyl ehter coordinating mixture at 220 °C. Different temperatures and duration of further heating were tested to control the size and the shape of $CoPt_3$ nanocrystals. The yield of the reaction was ∼0.035−0.040 g of properly washed $CoPt_3$ nanocrystals for all coordinating mixtures and temperature regimes.

Additional Injections of the Precursors. The method described above allows the preparation of $CoPt_3$ particles with sizes ranging from ∼1.5 to 5.5 nm, depending on reaction conditions and the compositions of coordinating mixture. To prepare larger $CoPt_3$ nanocrystals (up to ∼10 nm), additional injections of cobalt and platinum precursors into the reaction mixture were required. We used a solution of precursors prepared by mixing of relevant amounts of $Co_2(CO)_8$ (0.0225 g), $Pt(acac)_2$ (0.0164 g), 1,2-hexadecanediol (0.065 g), 1,2-dichlorobenzene (0.4 mL), and diphenyl ether (3.0 mL). This solution of precursors was dropwise introduced into the reaction mixture at 155 °C. After injection, the temperature was slowly (∼2 grad/min) increased up to 230 °C and heating was continued at this temperature for 40 min. All subsequent injections were carried out at the same conditions.

Postpreparative Procedures. After cooling the reaction mixture to 50 °C, all subsequent steps were performed in air. The crude solution of $CoPt_3$ nanoparticles was mixed with 5 mL of chloroform. Subsequently, 20 mL of ethanol were added, resulting in a black precipitate which was isolated by centrifugation. The almost colorless supernatant was discarded. The precipitate was redissolved in chloroform (∼5 mL) and filtered through a PTFE 0.2 μm filter. To wash out the excess of stabilizers, the nanocrystals were precipitated again by addition of ∼20 mL of ethanol and centrifuged. The resulting black precipitate containing $CoPt_3$ nanocrystals can be redissolved in various nonpolar solvents (toluene, hexane, and chloroform, etc.). The color of the solution was changed from black-brown to brown in accordance with the concentration of $CoPt_3$ nanocrystals. Absorption spectrum of $CoPt_3$ colloidal solution is shown in Supporting Information. A small amount (∼0.1 mg) of HDA can be added to nanocrystals prepared in TDPA−diphenyl ether coordinating mixture to improve their solubility.

When the synthesis described above yielded monodisperse samples, no further size selection was applied. If a distribution of nanocrystals size was observed, the conventional solvent/nonsolvent size selective precipitation technique[11] was applied. Hexane and ethanol were used as solvent and nonsolvent, respectively.

A summary of the preparation conditions is listed in Table 1 and is discussed in more details below.

Growing the Colloidal Crystals of $CoPt_3$ Nanoparticles. Monodisperse $CoPt_3$ nanocrystals prepared in HDA−diphenyl ether coordinating mixture were thoroughly washed from the excess of organics and redissolved in toluene in a concentration of about 2 mg/mL. $CoPt_3$ colloidal crystals were grown from this solution using the recently introduced three-layer technique of controlled oversaturation.[12] Glass tubes (30 cm in length and 0.5 cm in diameter) were filled with colloidal solutions of $CoPt_3$ nanocrystals to a height of 15 cm. Then the layers of propanol-2 (7 cm) and methanol (7 cm) were carefully added on top of the $CoPt_3$ colloidal solution. The crystallization of $CoPt_3$ nanocrystals into 3D colloidal crystals continued for approximately 2−3 weeks.

Apparatus. Powder X-ray diffraction (XRD), transmission electron microscopy (TEM), high-resolution TEM (HRTEM), and elemental analysis were used to characterize the nanocrystals. XRD measurements were performed on a Philips X'Pert diffractometer (Cu Kα radiation, variable entrance slit, Bragg−Brentano geometry, secondary monochromator). Samples for these measurements were prepared by dropping colloidal solutions of $CoPt_3$ nanocrystals in toluene on standard single crystal Si supports and evaporating the solvent. TEM and HRTEM images were obtained using a Philips CM-300 microscope operated at 300 kV. Samples for these measurements were prepared by depositing a drop of nanocrystal solution in toluene or hexane onto carbon-coated copper grids. The excess of solvent was wicked away with a filter paper, and the grids were dried in air. SEM images were obtained on Philips 515 scanning electron microscope. The elemental composition of the nanocrystals was obtained by inductively coupled plasma-atomic emission spectroscopy (ICP AES). For these measurements, $CoPt_3$ nanocrystals were thoroughly washed to remove most of the organic ligands and subsequently dissolved in the standard HCl/HNO_3 digesting solution.

Results and Discussion

Synthesis of $CoPt_3$ Nanocrystals. $CoPt_3$ nanocrystals were prepared via the simultaneous reduction of $Pt(acac)_2$ and thermodecomposition of $Co_2(CO)_8$ in the presence of organic molecules terminating the growth of Co−Pt bulk phases. A similar approach has been recently applied for the preparation of monodisperse FePt nanocrystals.[5] In this work the authors used a binary stabilizer mixture of oleic acid and oleylamine. For Co−Pt alloy nanocrystals this mixture resulted, however, in the formation of a product which was almost amorphous in XRD. This result is consistent with a recent finding of Park et al.[7b] who reported the formation of $CoPt_3$ particles with diameters below 1.8 nm under these conditions. In the case of

(11) Chemseddine, A.; Weller, H. *Ber. Bunsen-Ges. Chem.* **1993**, *97*, 636.

(12) (a) Talapin, D. V.; Shevchenko, E. V.; Kornowski, A.; Gaponik, N. P.; Haase, M.; Rogach, A. L.; Weller, H. *Adv. Mater.* **2001**, 13, 1868. (b) Shevchenko, E. V.; Talapin, D. V.; Kornowski, A.; Wiekhorst, F.; Kötzler, J.; Haase, M.; Rogach, A. L.; Weller, H. *Adv. Mater.* **2002**, *14*, 287.

pure Co nanoparticles Sun et al.[4b] assumed a strong binding of oleic acid to surface sites which greatly impeded the particles to growth. Our results also suggest a too strong complexation of the metal by this stabilizer. Various capping agents (TOPO, TOP, phosphonic acids, primary and secondary amines, fatty acids, and mixtures of these compounds) were systematically tested in order to prepare stable colloids of Co−Pt alloy nanocrystals. We found that high-quality nanocrystals in the reported size regime could only be obtained in the presence of 1-adamantanecarboxylic acid or 1-adamantanacetic acid.

The best results (with respect to control of nanoparticle size, monodispersity, crystallinity, and the reproducibility of the synthesis) were obtained with two-component mixtures of HDA−diphenyl ether and TDPA−diphenyl ether in the presence of ACA (see Table 1). In fact, HDA and TDPA have been previously applied in the synthesis of cadmium chalcogenide nanocrystals of controllable sizes and shapes.[13]

The use of the HDA−diphenyl ether coordinating mixture and injection of the cobalt stock solution at 100 °C generally allowed the synthesis of spherical $CoPt_3$ nanocrystals with sizes ranging from ∼4 to 5.5 nm. As an example, the size histogram of an as-prepared $CoPt_3$ nanocrystal sample with a mean size of 4.8 nm (standard deviation, 12%) is shown in the Supporting Information (Figure S2a). Under these reaction conditions some amount of nanowires were also formed as a side product, which could be easily removed by high-speed centrifugation or size selective precipitation (see details in the Supporting Information, Figures S3 and S4). The amount of wires and their length decreased drastically upon prolonged (∼3 h) refluxing (Supporting Information, Figure S3). More detailed studies of nanowire formation will be reported in a forthcoming paper.

Exclusively spherical $CoPt_3$ nanocrystals were formed in TDPA−diphenyl ether or HDA−1-hexadecanol. Analysis of the TEM images and the XRD data shows that the duration of heating had no pronounced influence on the size of the spherical nanocrystals. Thus, refluxing for 1 min, 40 min, and 3 h resulted in similar sizes and size distributions of the spherical $CoPt_3$ nanocrystals. The use of TDPA−diphenyl ether as the coordinating mixture yielded spherical $CoPt_3$ nanocrystals with smaller sizes ranging from ∼3 to 5 nm. $CoPt_3$ nanocrystals of ∼1.5−2 nm, the HRTEM images of which (as prepared after washing) are shown in Figure 1a, were obtained in HDA−1-hexadecanol. Subsequent size-selective precipitation allowed further narrowing of the size distribution.

When the cobalt stock solution was injected into the reaction mixture at higher temperature (170 °C instead of 100 °C), monodisperse spherical $CoPt_3$ nanocrystals with mean sizes of about 4 nm and ∼3.5 nm were obtained in HDA−diphenyl ether and TDPA−diphenyl ether, respectively. The corresponding TEM images are shown in Figure 1b (standard deviation, 9%; size histogram, see Supporting Information) and further below in Figure 3b,d. No postpreparative size selection was necessary to obtain the narrow particle size distribution in this case. A similar effect of narrowing the particle size distribution was observed for so-called "hot injection" technique in the synthesis of CdSe and InAs nanocrystals.[14] Usually, the monodisperse

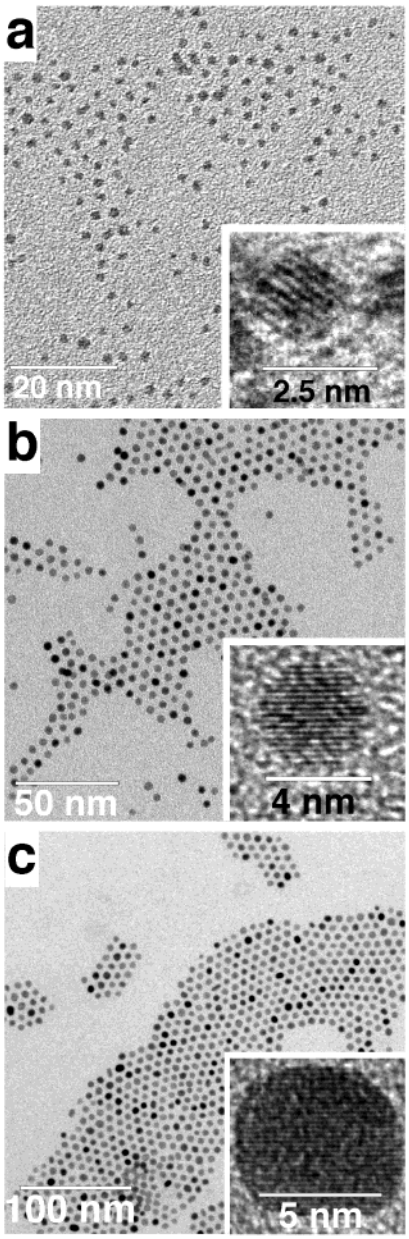

Figure 1. TEM overview of 1.5 (a), 3.8 (b), and 6.2 nm (c) $CoPt_3$ nanocrystals. Insets show HRTEM image of each size.

$CoPt_3$ nanocrystals spontaneously formed 3D arrays on the TEM grids, making the estimation of standard deviation in such cases difficult. Counting the lattice planes of individual nanocrystals in HRTEM images provides very high monodispersity within the self-assembled domains.

Additional injections of platinum and cobalt precursors into the solutions of the $CoPt_3$ nanoparticles prepared in HDA−diphenyl ether or TDPA−diphenyl ether coordinating mixtures increased the mean size while keeping the size distribution still narrow. Figure 1c presents ∼6.2 nm (standard deviation, 12%) $CoPt_3$ nanocrystals obtained from monodisperse 4.0 nm $CoPt_3$ nanocrystals by one additional injection of the corresponding amount of precursors (size histogram is shown in Supporting Information, Figure S2c). Obviously, the 4 nm particles acted as nucleation seeds for the deposition of the additional monomer. However, more than two additional injections led to a substantial broadening of the size distribution and formation of ∼10 nm

(13) (a) Talapin, D. V.; Rogach, A. L.; Kornowski, A.; Haase, M.; Weller, H. *Nano Lett.* **2001**, *1*, 207. (b) Peng, Z. A.; Peng, X. *J. Am. Chem. Soc.* **2001**, *123*, 183.
(14) Peng, X.; Wickham, J.; Alivisatos, A. P. *J. Am. Chem. Soc.* **1998**, *120*, 5343.

irregular-shaped polycrystalline $CoPt_3$ nanocrystals (Supporting Information, Figure S5).

To further elucidate the role of ACA, had, and TDPA in the respective reaction mixtures, we either removed one component completely during the synthesis or added it at a later stage of preparation. These experiments were performed using diphenyl ether as the solvent, and the results can be summerized as follows: Using only ACA as stabilizer also allowed the synthesis of crystalline $CoPt_3$ nanoparticles, exhibiting, however, a rather broad size distribution and a rather poor colloidal stability; i.e., these particles precipitated within 1 day after the final redissolution step (see postpreparative procedures). The resulting precipitate could not be redissolved by an access of ACA, whereas addition of HDA or dodecylamine resulted in an immediate and TDPA in a slow formation of a clear colloidal solution. On the other hand, when ACA was removed from the reaction mixture and only amines or TDPA were used from the beginning, a black precipitate of bulk Co and Pt was formed which could not be redissolved by any postpreparative treatment. We therefore conclude that ACA has the main influence on the formation and stabilization of $CoPt_3$ nanocrystals, whereas amines and phosphonic acid work as cosurfactants improving the stability and size distrubution of the resulting nanocrystals. We assume that HDA is the object of a reversible, dynamic surface eqillibrium. This assumption is supported by the observation that repeated washing with ethanol results in precipitation of $CoPt_3$ nanocrystals, which, however, can easily be redissolved after renewed addition of HDA.

It appears feasible to connect the extraordinary role of ACA with the bulky adamantyl end groups. In contrast to linear chains these adamantyl groups will probably protect a number of free surface sites from being coordinated by ligand molecules and, thus, increase the free surface energy. This explains why the particles grow to larger sizes and crystallization easily occurs in contrast to experiments with fatty acids.

ATR-FTIR investigations were carried in order to verify the postulated surface chemistry. Unfortunately, these spectra were strongly dominated by CH vibrations which can hide additional information about interaction behavior of ACA TDPA with the surface of $CoPt_3$ nanocrystals. Although slightly shifted bands of the carboxylic acid groups (COO^-) could be detected at $\nu =$ 1600 and 1450 cm^{-1}, an unambigious interpretation of possible binding sites is presently not possible. Amine stretching bands, as present in the spectrum of pure HDA, could not be detected in the samples of our nanocrystals.

In another set of blank experiments we tried the preparation of pure Co and pure Pt nanoparticles by removing the respective precursor under identical reaction conditions. As a result, we obtained a transparent blue solution in the case of prolonged heating of cobalt carbonyl without any traces of crystalline material, whereas the respective experiment with $Pt(acac)_2$ resulted in the formation of bulk fcc platinum which precipitated immediately. This behavior can be explained with strong difference in the binding energy of ACA to Co and Pt and suggests that ACA preferentially binds to Co. In this sense at least two types of surface sites of $CoPt_3$ nanocrystals can be proposed. Another explanation involves strong differences in the lattice energies of Co and Pt nanoparticles.

Structural Characterization of $CoPt_3$ Nanocrystals. ICP AES measurements showed the ratio between Co and Pt being close to 1:3 for all samples studied. EDX measurements indicated the same compositions.

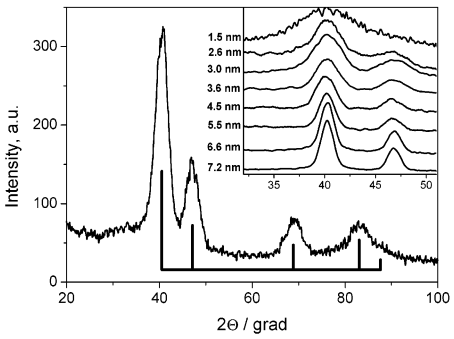

Figure 2. XRD pattern of as-synthesised 4.0 nm $CoPt_3$ nanocrystals (reflexes of bulk fcc $CoPt_3$ are shown with a stick spectrum). Inset: Size-dependent XRD. The size of the nanocrystals was calculated by the Debye−Sherrer equation.

HRTEM images (insets in Figure 1a−c) of differently sized $CoPt_3$ nanocrystals show crystalline particles with clearly resolved lattice fringes and almost no distortions within nanocrystal cores. XRD patterns of as-prepared nanocrystals (Figure 2) corresponded to the chemically disordered face-centered cubic (fcc) $CoPt_3$ structure which was also observed for vapor-deposited Co_xPt_{1-x} films.[10d] The width of the diffraction peaks at wide angles was considerably broadened and increased with decreasing particle size (Figure 2, inset). The intensity pattern of the reflexes and the lattice constant were very close to that of bulk $CoPt_3$ phase[15] and showed that nanocrystals did not grow in a preferred direction. Particle sizes calculated from the peak widths agreed well with the sizes observed in the TEM images, indicating a very high degree of average particle crystallinity; i.e., the particles represent single crystalline domains.

Although the XRD patterns are in good agreement with $CoPt_3$, nanophase segregation or even core−shell formation cannot completely be excluded from these data. We believe, however, that these processes do not occur under our reaction conditions, for the following reasons: Because of its much lower contrast, domains of pure Co should be recognized in TEM against a background of Pt or $CoPt_3$. Contrarily, segregated Pt domains cannot be distinguished from $CoPt_3$ by TEM because of the similarity in phase contrast and lattice spacing. To get more evidence for single phase formation, we varied the ratio between Co and Pt precursors during the synthesis and measured the elemental composition of the isolated nanoparticles by ICP AES and XRD. In all cases we found a composition very close to $CoPt_3$. Thus, the behavior of the pure elementary compounds (Co and Pt) as well as the constant stoichiometry observed for the obtained nanocrystals rule out the possibility of nanophase segregation or core−shell formation from our point of view.

Self-Assembly of $CoPt_3$ Nanocrystals. Due to their narrow particle size distributions and the uniform spherical shape, the $CoPt_3$ nanocrystals had a strong tendency to self-organize into 2D and 3D superlattices. Spontaneous self-assembly was observed when colloidal solutions of $CoPt_3$ nanocrystals were spread onto a substrate with subsequent slow evaporating of the carrier solvent. Depending on the particle size and conditions of solvent evaporation, several kinds of self-organized superstructures were observed. Thus, Figure 3a shows a TEM overview image of a close-packed monolayer of 4.8 nm $CoPt_3$

(15) Geisler, A. H.; Martin, D. L. *J. Appl. Phys.* **1952**, *23*, 375.

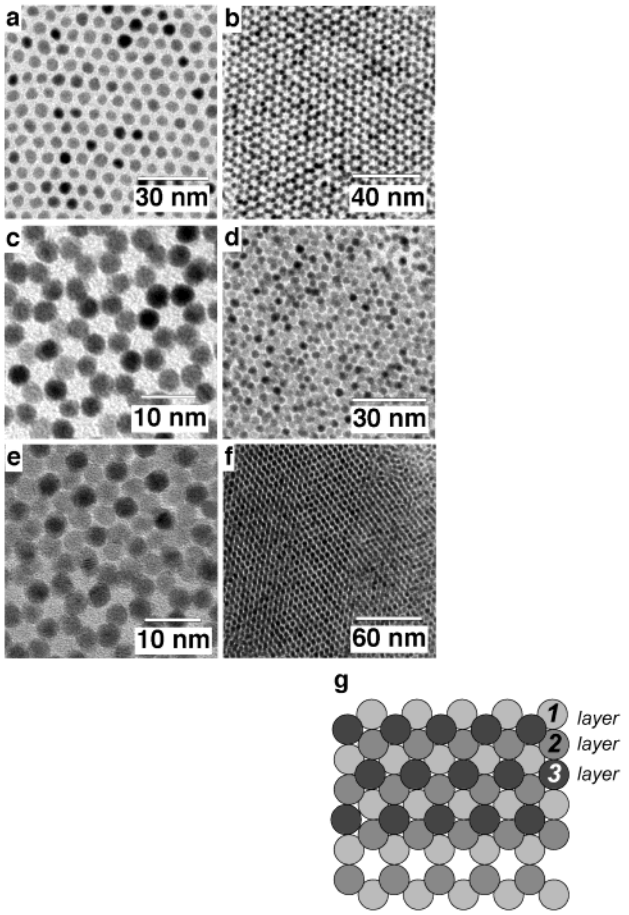

Figure 3. TEM images (a) of monolayer of 4.8 nm $CoPt_3$ nanoparticles, (b, c) of two layers of 3.6 and 4.0 nm $CoPt_3$ nanoparticles, (d) of three layers of 3.6 nm $CoPt_3$ nanoparticles, (e) of three layers of 4.0 nm $CoPt_3$ nanoparticles (HRTEM), (f) of more than five layers of 4.5 nm $CoPt_3$ nanoparticles and a graphical illustration (g) of three-layer arragement of $CoPt_3$ nanocrystals.

nanocrystals. If the surface coverage with nanocrystals was higher than one monolayer, nanocrystals of the second layer occupied positions between the nanocrystals in the first layer (Figure 3b,c). Due to the relatively large interparticle spacing of ~2.5 nm presumably maintained by the bulky ACA capping ligands, two layers of $CoPt_3$ nanocrystals form the above-mentioned structure observable for different nanocrystal sizes (Figure 3b,c). The third layer of nanocrystals occupied the positions typical for cubic close packing ccp (Figure 3d,e). Figure 3e gives a magnified image of a three-layered assembly of 4.0 nm $CoPt_3$ nanocrystals. The difference in phase contrast between two underlying layers and a darker third layer allows us to attribute each nanocrystal to the layer it is placed in and permits us to conclude that $CoPt_3$ nanocrystals are packed into ccp-like superlattice, where the nanocrystals are separated from each other by thick (2.5 nm) organic shells. Figure 3f presents a TEM image of multilayer 3D superlattice where the 4.5 nm $CoPt_3$ nanocrystals are arranged in a nearly defect-free 3D structure exhibiting long-range order. Graphical illustration (Figure 3g) clarifies the three-layer arrangement of $CoPt_3$ nanocrystals.

Two-dimensional superlattices built from the monodisperse nanocrystals of two different sizes were recently reported.[16] Au or Ag and Au nanoparticles organized themselves in regular AB_2 or AB alloy superstructures, depending on the relative

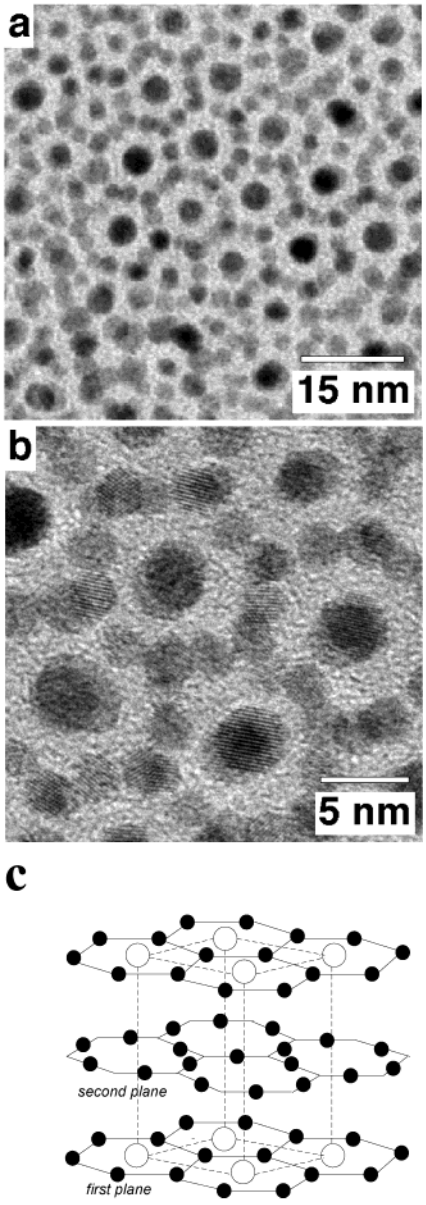

Figure 4. (a) TEM and (b) HRTEM images illustrating 3D superlattices of $CoPt_3$ nanoparticles formed in a mixture of two different sizes (4.5 and 2.6 nm); (c) illustrative drawing of the AB_5 structure.

amount of each species and the ratio of particle diameters. Mixing two monodisperse colloids of $CoPt_3$ nanocrystals (4.5 and 2.6 nm diameter) followed by slow evaporation of the solvent, a 3D superlattice was obtained (Figure 4a,b). These images correspond to a view along the *c*-axis of a three layer assembly, the structure of which is depicted in Figure 4c. It represents the crystal structure of the intermetallic compound $CaCu_5$ [17] (AB_5 type). This structure was also observed in a superlattice formed by latex globules.[18] In the first plane each 4.5 nm $CoPt_3$ nanocrystal is surrounded by a hexagon formed from 2.6 nm nanocrystals. The second plane consists only of hexagons of small particles, which are, however, rotationally

(16) (a) Kiely, C. J.; Fink, J.; Brust, M.; Bethell, D.; Schiffrin, D. J. *Nature* **1998**, *396*, 444. (b) Kiely, C. J.; Fink, J.; Zheng, J. G.; Brust, M.; Bethell, D.; Schiffrin, *Adv. Mater.* **2000**, *12*, 640.
(17) Pearson, W. B. *Crystal Chemistry and Physics of Metals and Alloys 643*; Wiley-Interscience: London, 1972.
(18) (a) Hachisu, S.; Youshimura, S. *Nature* **1980**, *283*, 188. (b) Youshimura, S.; Hachisu, S. Prog. *Colloid Polym. Sci.* **1983**, *68*, 59.

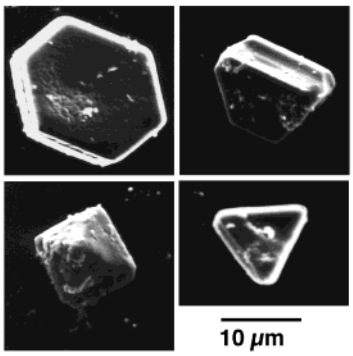

Figure 5. SEM images of colloidal crystals of $CoPt_3$ nanoparticles illustrating their different shapes.

shifted by 30° relative to the first plane, and the third plane repeats the first one.

The formation of 3D colloidal crystals was observed for CdS,[19] CdSe,[12a,20] and FePt[12b] nanoparticles. In these colloidal structures monodisperse nanocrystals play the role of building blocks and can be considered artificial atoms in the next level of hierarchy. Monodisperse $CoPt_3$ nanocrystals have a strong tendency to form 3D superlattices, as evidenced from Figure 3. Applying the recently introduced controlled oversaturation technique[12] allowed us to grow colloidal crystals also from $CoPt_3$ nanoparticles. SEM images (Figure 5) show such well-facetted hexagonal, triangular, and pyramid-like colloidal crystals reaching sizes of tens of micrometers.

Temporal Stability and Thermostability of $CoPt_3$ Nanocrystals. Long-term stability under ambient conditions is an important issue for any new nanomaterial, especially for its potential application. Colloidal solutions prepared by washing and redissolving $CoPt_3$ nanocrystals in nonpolar solvents (hexane, toluene, or chloroform) were stable for several days before a uniform film was formed at the bottom and the walls of the glass vessel. Addition of small amounts of HDA (~0.1 mg of HDA/(25 mg of the nanocrystals)) resulted in immediate dissolution of this film. The resulting colloids were stable in air for months without any further precipitation. XRD patterns of the samples which were stored in air for weeks were almost identical to those of as-prepared $CoPt_3$ nanocrystals. Even at elevated temperatures oxidation of $CoPt_3$ nanocrystals was very slow. Figure 6a shows XRD patterns of both as-prepared $CoPt_3$ nanocrystals, and the samples annealed at 100, 200, and 300 °C for 2 h in air. The nanocrystals annealed at 100 and 200 °C were still easily soluble in nonpolar solvents and did not reveal the presence of any oxides. After being annealed at 300 °C in air, the $CoPt_3$ nanocrystals became insoluble in common nonpolar solvents and the XRD pattern revealed weak additional reflexes which could be assigned to CoO. Moreover, the (111) reflex in the XRD pattern was slightly shifted toward a platinum-rich alloy. XRD patterns of $CoPt_3$ samples annealed at 400 and 500 °C under vaccum did not show the presence of any crystalline oxides as well (Figure 6b).

Summary

A colloidal synthesis of $CoPt_3$ nanoparticles was developed for the first time allowing the preparation of particles of different distinct sizes (from 1.5 to 7.2 nm) with narrow particle size distribution. The key point of the synthesis is the use of the novel stabilizer 1-adamantancarboxylic acid. Elemental analysis, XRD data, and TEM and HRTEM images provided direct prove of the formation of highly crystalline $CoPt_3$ nanoparticles possessing a chemically disordered fcc structure. The $CoPt_3$ nanocrystals were stable in air and did not reveal any oxidation even after annealing at 200 °C under ambient conditions. Nearly spherical $CoPt_3$ nanocrystals had a strong tendency to form 2D and 3D superstructures, which is of particular importance for their practical application. Three-dimensional superlattices of AB_5 type were observed for a binary mixture of $CoPt_3$ nanocrystals of two different sizes. Perfectly facetted ~10−20 μm colloidal crystals consisting of monodisperse $CoPt_3$ nanocrystals were prepared using the three-layer technique of controlled oversaturation. Under certain reaction conditions the formation of $CoPt_3$ nanowires was observed. The mechanism of the formation of nanowires and magnetic properties of $CoPt_3$ nanocrystals are currently under investigation.

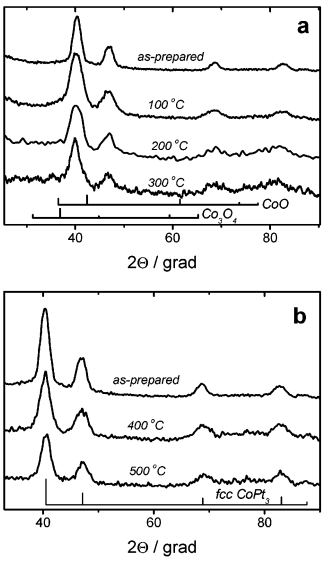

Figure 6. (a, b) XRD patterns of annealed $CoPt_3$ nanoparticles (a) in air and (b) under vacuum, respectively.

Acknowledgment. We thank Prof. Dr. S. Förster, Dr. N. Gaponik, and Dr. K.-H. Klaska for helpful discussions, Prof. Dr. J. Kötzler and F. Wiekhorst for magnetic measurement of our samples, Dr. E. Geidel for ATR FTIR investigations, J. Kolny for assistance with XRD measurements, and I. Ralya and S. Bartholdi-Nawrath for assistance with the SEM and TEM measurements, respectively. This work was supported in part by the EU research project BIOAND.

Supporting Information Available: Absorption spectrum of $CoPt_3$ nanocrystals (Figure S1), size histogram of as-prepared 4.8, 3.8, and 6.2 nm (Figure S2), TEM and HRTEM images of nanowires (Figures S3 and S4), TEM image of polydisperse polycrystalline $CoPt_3$ nanocrystals obtained by three additional injections (Figure S5), magnetization vs field measurements and ZFC/ZF temperature dependencies of the magnetization in a field of 100 Oe measured on ~6.2 nm $CoPt_3$ nanocrystals (Figure S6) (PDF). This material is available free of charge via the Internet at http://pubs.acs.org.

JA025976L

(19) (a) Vossmeyer, T.; Reck, G.; Katsikas, L.; Haupt, E. T. K.; Schulz, B.; Weller, H. *Science* **1995**, *267*, 1476. (b) Vossmeyer, T.; Reck, G.; Schulz, B.; Katsikas, L.; Weller, H. *J. Am. Chem. Soc.* **1995**, *117*, 12881.
(20) Murray, C. B.; Kagan, C. R.; Bawendi, M. G. *Science* **1995**, *70*, 1335.